Article

Synthesis and Evaluation of ^{99m}Tc-labeled PSMA-targeted Tracers Based on the Lys-urea-Aad Pharmacophore for Detecting Prostate Cancer with Single Photon Emission Computed Tomography

Kelly Lu [1], Chengcheng Zhang [1], Zhengxing Zhang [1], Hsiou-Ting Kuo [1], Nadine Colpo [1,2], François Bénard [1,2,3] and Kuo-Shyan Lin [1,2,3,*]

[1] Department of Molecular Oncology, BC Cancer Research Institute, Vancouver, BC V5Z 1L3, Canada; klu@bccrc.ca (K.L.); cczhang@bccrc.ca (C.Z.); zx1981ok@hotmail.com (Z.Z.); hkuo@bccrc.ca (H.-T.K.); ncolpo@bccrc.ca (N.C.); fbenard@bccrc.ca (F.B.)
[2] Department of Functional Imaging, BC Cancer, Vancouver, BC V5Z 4E6, Canada
[3] Department of Radiology, University of British Columbia, Vancouver, BC V5Z 1M9, Canada
* Correspondence: klin@bccrc.ca (K.-S.L.)

Abstract: Prostate-specific membrane antigen (PSMA) is a well validated prostate cancer marker, but reported PSMA-targeted tracers derived from the Lys-urea-Glu pharmacophore including the clinically validated [^{99m}Tc]Tc-EDDA/HYNIC-iPSMA have high off-target uptake in kidneys, spleen and salivary glands. In this study, we synthesized and evaluated three novel ^{99m}Tc-labeled PSMA-targeted tracers and investigated if the tracers derived from the Lys-urea-Aad pharmacophore could have minimized uptake in off-target organs/tissues. *In vitro* competition binding assays showed that compared with HYNIC-iPSMA, the three novel ligands had slightly weaker PSMA binding affinity (average K_i = 3.11 vs 8.96 - 11.6 nM). Imaging and *ex vivo* biodistribution studies in LNCaP tumor-bearing mice showed that [^{99m}Tc]Tc-EDDA/HYNIC-iPSMA and the three novel tracers successfully visualized LNCaP tumor xenografts in SPECT images and were excreted mainly via the renal pathway. The average tumor uptake at 1 h post-injection varied from 5.40 to 18.8 %ID/g, and the tracers derived from the Lys-urea-Aad pharmacophore had much lower uptake in spleen and salivary glands. Compared with the clinical tracer [^{99m}Tc]Tc-EDDA/HYNIC-iPSMA, the Lys-urea-Aad derived [^{99m}Tc]Tc-EDDA-KL01127 had lower background uptake and superior tumor-to-background contrast ratios, and is therefore promising for clinical translation to detect prostate cancer lesions with SPECT.

Keywords: prostate-specific membrane antigen (PSMA); technetium-99m; single photon emission computed tomography (SPECT); molecular imaging; HYNIC

1. Introduction

Prostate cancer (PCa) is one of the leading causes of cancer mortality in men worldwide. Currently, its incidence and mortality have plateaued potentially due to limitations of current diagnostic and therapeutic options for PCa [1]. Hence, more effective molecular and functional-based imaging using radiotracers targeting PCa markers may provide enhanced diagnosis and monitoring of the disease. Prostate-specific membrane antigen (PSMA), also known as glutamate carboxypeptidase II (GCPII), is a biomarker expressed on epithelial prostate cells but found to be overexpressed in PCa and its expression correlates with disease progression, recurrence, metastasis, and survival even in patients with castration-resistance PCa [2–4].

PSMA features an extracellular active site which catalyzes the hydrolysis of *N*-acetyl-aspartyl-glutamate into *N*-acetyl-aspartate and glutamate, and is also the binding site of most currently reported PSMA-targeted small molecules [5,6]. Among PSMA inhibitors, urea-based small molecules provide stability and an opportunity for cell internalization, and have been extensively explored as

Preprints (www.preprints.org) | NOT PEER-REVIEWED | Posted: 8 June 2023 doi:10.20944/preprints202306.0605.v1

PSMA-targeted tracers for positron emission tomography (PET) imaging such as [^{18}F]DCFPyL and [^{68}Ga]Ga-PSMA-11 (Figure 1) to single photon emission computed tomography (SPECT) imaging such as [^{99m}Tc]Tc-EDDA/HYNIC-iPSMA (Figure 1). These reported PSMA-targeted tracers all share the same lysine-urea-glutamate (Lys-urea-Glu, in brown, Figure 1) pharmacophore [7,8]. However, a limitation to utilizing the Lys-urea-Glu pharmacophore is the off-target accumulation in some normal organs/tissues including kidneys, spleen, salivary glands and liver, which could deter detection of metastatic PCa lesions in or adjacent to these organs/tissues [9,10]. Our previous work demonstrated that a PSMA-targeted PET tracer, [^{68}Ga]Ga-HTK03149 (Figure 1), derived from a modified lysine-urea-aminoadipic acid (Lys-urea-Aad) pharmacophore had minimal uptake in the commonly reported off-target organs including kidneys, spleen, salivary glands and liver [11]. Hence the goal of this study is to investigate if the same effect could be observed on the development of ^{99m}Tc-labeled tracers for SPECT imaging.

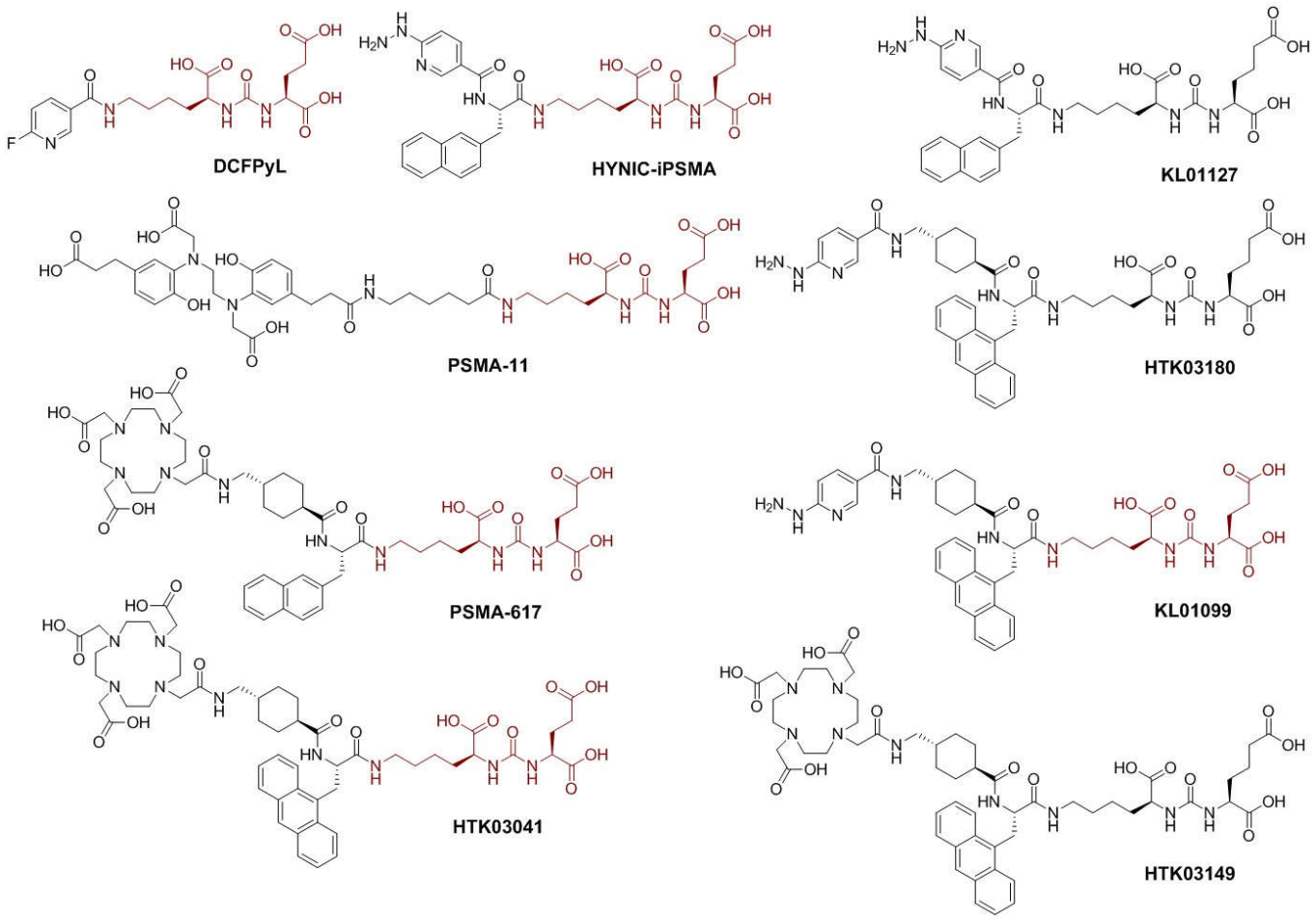

Figure 1. Chemical structures of PSMA-targeted ligands. The Lys-urea-Glu pharmacophore is in brown.

Despite higher sensitivity and spatial resolution of PET, SPECT is more readily available and accessible at hospital settings. Therefore, an optimized PSMA-targeted SPECT tracer especially labeled with ^{99m}Tc could have a wider applicability than the FDA-approved PET tracers, [^{18}F]DCFPyL and [^{68}Ga]Ga-PSMA-11. Moreover, ^{99m}Tc-based radiopharmaceuticals are easy to prepare from kit formulations and feature a longer half-life (6 h) for efficient utilization.

The clinically validated [^{99m}Tc]Tc-EDDA/HYNIC-iPSMA features a hydrazinonicotinamide (HYNIC) chelator which utilizes the co-ligand, ethylenediamine-*N*,*N*'-diacetic acid (EDDA) to complete the coordination of technetium under relatively mild conditions that can be facilely developed into freeze-dried kit formulation for clinical use [12–14]. Despite its capability to detect PSMA-expressing PCa lesions, high uptake of [^{99m}Tc]Tc-EDDA/HYNIC-iPSMA was also observed in the reported off-targets of other PSMA-targeted tracers including salivary glands, liver, kidneys and

Preprints (www.preprints.org) | NOT PEER-REVIEWED | Posted: 8 June 2023 doi:10.20944/preprints202306.0605.v1

spleen. Therefore, in this study we used [^{99m}Tc]Tc-EDDA/HYNIC-iPSMA as a template and investigated if (1) replacing the PSMA-targeted Lys-urea-Glu pharmacophore with the Lys-urea-Aad pharmacophore could lead to new derivatives with lower off-target uptake in normal organs, and (2) optimizing the selection of linker between the PSMA-targeted pharmacophore and the HYNIC chelator could lead to new derivatives with higher PSMA binding affinity and/or higher uptake in PSMA-expressing PCa cancer tumor xenografts.

As shown in Figure 1, we synthesized HTK03180, KL01099 and KL01127, and compared the performance of their ^{99m}Tc-labeled complexes with [^{99m}Tc]Tc-EDDA/HYNIC-iPSMA. HYNIC-iPSMA is a derivative of PSMA-617 (Figure 1) by replacing the DOTA-tranexamic acid moiety with the HYNIC chelator. Previously, we demonstrated that tranexamic acid is crucial for high binding affinity to PSMA [15]. Therefore, we preserved tranexamic acid as part of the lipophilic liker for HTK03180 and KL01099. Previously, we also demonstrated that replacing the 2-naphthylalanine in [^{68}Ga]Ga-PSMA-617 with 9-anthrylalaine resulted in [^{68}Ga]Ga-HTK03041 (Figure 1) which had higher PSMA binding affinity and uptake in PSMA-expressing LNCaP tumor xenografts than [^{68}Ga]Ga-PSMA-617 [16]. We would like to investigate if the same effect could be observed in ^{99m}Tc-labeled HYNIC-conjugated tracers (HTK03180 and KL01099, Figure 1). Lastly, instead of the traditional PSMA-targeted Lys-urea-Glu pharmacophore in HYNIC-iPSMA and KL01099, we had the Lys-urea-Aad pharmacophore in HTK03180 and KL01127. This was to investigate if the ^{99m}Tc-labeled tracer derived from the Lys-urea-Aad pharmacophore could have lower off-target uptake in normal organs than its Lys-urea-Glu analog (HTK03180 vs KL01099 and HYNIC-iPSMA vs KL01127, Figure 1).

2. Results

2.1. Synthesis of PSMA-targeted ligands and their Tc-99m labeled analogs

PSMA-targeted ligands including HYNIC-iPSMA, HTK03180, KL01099 and KL01127 were constructed on solid phase and obtained in 18 - 36% yield after HPLC purification. Their Tc-99m labeled analogs were obtained in 63 – 89% decay-corrected radiochemical yield with > 97% radiochemical purity and > 55 GBq/μmol molar activity.

2.2. PSMA binding affinity and hydrophilicity

All tested PSMA-targeted ligands inhibited the binding of [^{18}F]DCFPyL to PSMA-expressing LNCaP cells in a concentration-dependent manner (Figure 2, n = 3). Their calculated K_i values were in nM range ranking from the highest binding with HYNIC-iPSMA (3.11 ± 0.76 nM), followed by KL01127 (8.96 ± 0.58 nM), KL01099 (10.71 ± 0.21 nM), and HTK03180 (11.6 ± 1.5 nM). HYNIC-iPSMA has a significantly higher binding affinity than the other three ligands (ANOVA, $p < 0.001$), whereas there is no significant difference between the binding affinities of KL01127, KL01099 and HTK03180 (ANOVA, $p > 0.05$).

Preprints (www.preprints.org) | NOT PEER-REVIEWED | Posted: 8 June 2023 doi:10.20944/preprints202306.0605.v1

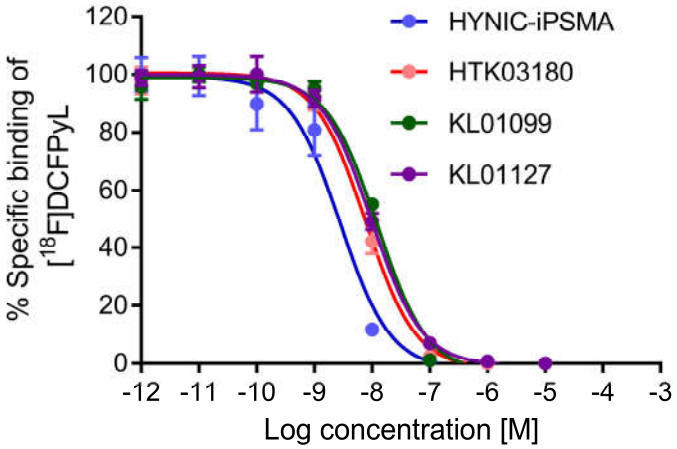

Figure 2. Inhibition of [^{18}F]DCFPyL binding to PSMA-expressing LNCaP cells by various concentrations of HYNIC-iPSMA, HTK03180, KL01099, and KL01127 .

The hydrophilicity of the ^{99m}Tc-labeled tracers was measured via the shake-flask method with the $LogD_{7.4}$ values calculated to be -3.31 ± 0.02, -2.56 ± 0.02, -2.14 ± 0.01, and -3.37 ± 0.11 (n = 3) for [^{99m}Tc]Tc-EDDA/HYNIC-iPSMA, [^{99m}Tc]Tc-EDDA-HTK03180, [^{99m}Tc]Tc-EDDA-KL01099, and [^{99m}Tc]Tc-EDDA-KL01127, respectively. Analyses by *t*-test reveal that [^{99m}Tc]Tc-EDDA-HTK03180 is more hydrophilic than [^{99m}Tc]Tc-EDDA-KL01099 (-2.56 ± 0.02 vs -2.14 ± 0.01; $p < 0.01$), whereas no difference is observed between [^{99m}Tc]Tc-EDDA/HYNIC-iPSMA and [^{99m}Tc]Tc-EDDA-KL01127 (-3.31 ± 0.02 vs -3.37 ± 0.11; $p > 0.1$).

2.3. Ex vivo biodistribution and SPECT/CT imaging studies

Representative SPECT/CT images of the investigated ^{99m}Tc-labeled PSMA-targeted tracers in LNCaP tumor-bearing mice are shown in Figure 3. All tracers successfully visualized LNCaP tumor xenografts in SPECT images with good contrast, and were excreted mainly via the renal pathway. [^{99m}Tc]Tc-EDDA/HYNIC-iPSMA (Figure 3A), [^{99m}Tc]Tc-EDDA-HTK03180 (Figure 3B) and [^{99m}Tc]Tc-EDDA-KL01127 (Figure 3D) had high tumor uptake, and [^{99m}Tc]Tc-EDDA-KL01099 (Figure 3C) had a relatively lower tumor uptake. [^{99m}Tc]Tc-EDDA/HYNIC-iPSMA, [^{99m}Tc]Tc-EDDA-HTK03180 and [^{99m}Tc]Tc-EDDA-KL01099 had very high uptake in kidneys, but only moderate kidney uptake was observed by using [^{99m}Tc]Tc-EDDA-KL01127. The tumor uptake of [^{99m}Tc]Tc-EDDA-KL01127 was sustained over time while its kidney uptake was slightly reduced from 1 h to 3 h post-injection. The tumor and kidney uptake of [^{99m}Tc]Tc-EDDA-KL01127 and [^{99m}Tc]Tc-EDDA-HTK03180 was greatly reduced with co-injection of the PSMA inhibitor 2-(phosphonomethyl)pentanedioic acid (2-PMPA, 0.5 mg).

Preprints (www.preprints.org) | NOT PEER-REVIEWED | Posted: 8 June 2023 doi:10.20944/preprints202306.0605.v1

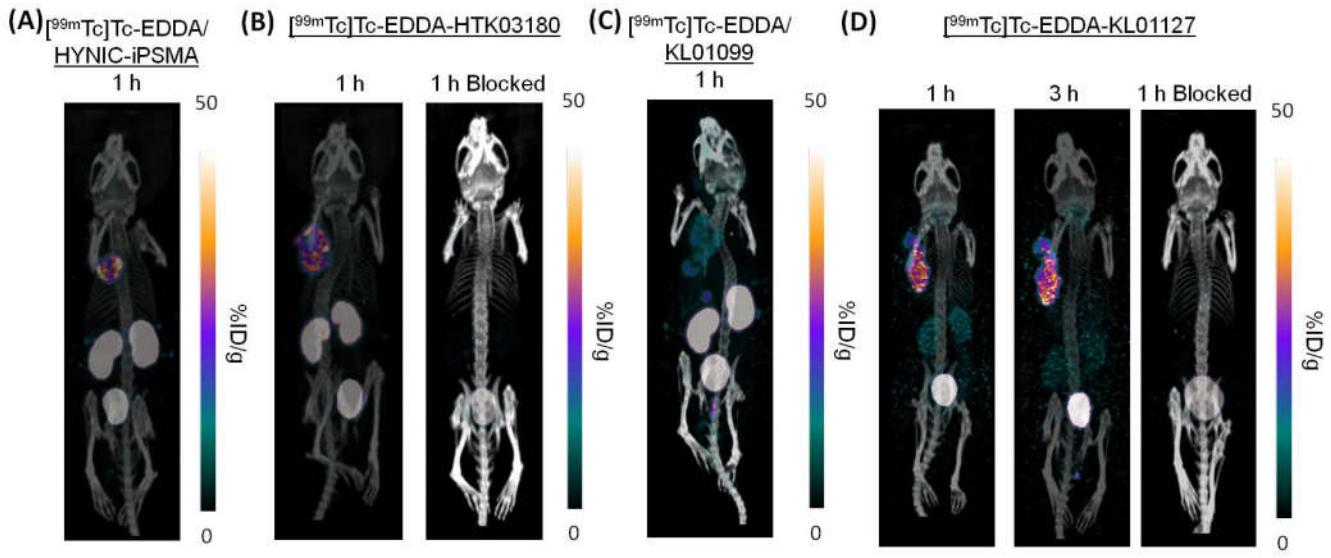

Figure 3. Representative SPECT/CT images with LNCaP tumour in the left shoulder of (A) [^{99m}Tc]EDDA/HYNIC-iPSMA, (B) [^{99m}Tc]Tc-EDDA-HTK03180, (C) [^{99m}Tc]Tc-EDDA-KL01099 and (D) [^{99m}Tc]Tc-EDDA-KL01127 in LNCaP tumor-bearing mice. The mice in the blocked groups were co-injected with 0.5 mg of 2-PMPA.

The biodistribution data of these PSMA-targeted tracers presented in Table 1 are consistent with the observations from their SPECT images. The tumor uptake values of [^{99m}Tc]Tc-EDDA/HYNIC-iPSMA, [^{99m}Tc]Tc-EDDA-HTK03180, [^{99m}Tc]Tc-EDDA-KL01099, and [^{99m}Tc]Tc-EDDA-KL01127 at 1 h post-injection were 10.3 ± 2.76, 18.8 ± 6.71, 5.36 ± 1.18, and 9.48 ± 3.42 %ID/g, respectively, and their kidney uptake values were 45.3 ± 20.5, 91.8 ± 29.1, 65.9 ± 5.10, and 15.0 ± 14.7 %ID/g, respectively. The spleen uptake at 1 h post-injection was higher for the tracers derived from the Lys-urea-Glu pharmacophore (23.4 ± 6.40 %ID/g for [^{99m}Tc]Tc-EDDA/HYNIC-iPSMA and 20.6 ± 7.77 %ID/g for [^{99m}Tc]Tc-EDDA-KL01099) than the tracers derived from the Lys-urea-Aad pharmacophore (3.14 ± 1.43 %ID/g for [^{99m}Tc]Tc-EDDA-HTK03180 and 0.23 ± 0.03 %ID/g for [^{99m}Tc]Tc-EDDA-KL01127). Similarly, the salivary gland uptake at 1 h post-injection was also higher for the tracers derived from the Lys-urea-Glu pharmacophore (7.77 ± 3.01 %ID/g for [^{99m}Tc]Tc-EDDA/HYNIC-iPSMA and 19.1 ± 4.05 %ID/g for [^{99m}Tc]Tc-EDDA-KL01099) than the tracers derived from the Lys-urea-Aad pharmacophore (2.35 ± 0.15 %ID/g for [^{99m}Tc]Tc-EDDA-HTK03180 and 0.25 ± 0.19 %ID/g for [^{99m}Tc]Tc-EDDA-KL01127). All tracers had minimal uptake (< 2.2 %ID/g) in liver and intestines, indicating their excretions were mainly via the renal pathway. Among these tracers, [^{99m}Tc]-EDDA-HYNIC-KL01127 had the highest tumor-to-background contrast ratios at 1 h post-injection (80.7 ± 42.7, 97.0 ± 42.9, 18.5 ± 3.54 and 0.87 ± 0.39 for tumor-to-bone, tumor-to-muscle, tumor-to-blood and tumor-to-kidney ratio, respectively). The tumor-to-background contrast ratios of [^{99m}Tc]-EDDA-HYNIC-KL01127 further increased from 1 h to 3 h post-injection due to a relatively sustained tumor uptake (9.48 ± 3.42 to 7.58 ± 2.48 %ID/g) but greatly reduced uptake in most of the background organs/tissues. Co-injection of [^{99m}Tc]Tc-EDDA-HTK03180 with 2-PMPA (0.5 mg) significantly reduced its average uptake in spleen, kidneys, LNCaP tumor xenograft and salivary glands by 85, 95, 95 and 70%, respectively. Similarly, co-injection of [^{99m}Tc]Tc-EDDA-KL01127 with 2-PMPA (0.5 mg) also significantly reduced its uptake in spleen, kidneys, LNCaP tumor xenograft and salivary glands by 43, 92, 95 and 32%, respectively.

Preprints (www.preprints.org) | NOT PEER-REVIEWED | Posted: 8 June 2023 doi:10.20944/preprints202306.0605.v1

Table 1. Uptake of ^{99m}Tc-labeled PSMA-targeted tracers in LNCaP-tumor bearing mice. The mice in the blocked groups were co-injected with 0.5 mg of 2-PMPA.

Organ Uptake (%ID/g)	[^{99m}Tc]Tc-EDDA/ HYNIC-iPSMA	[^{99m}Tc]Tc-EDDA-HTK03180		[^{99m}Tc]Tc-EDDA-KL01099	[^{99m}Tc]Tc-EDDA-KL01127		
	1 h (n = 4)	1 h (n = 5)	1 h Blocked (n = 4)	1 h (n = 4)	1 h (n = 5)	3 h (n = 5)	1 h Blocked (n = 4)
Blood	0.64 ± 0.11	1.33 ± 0.25	1.98 ± 0.28	0.81 ± 0.14	0.54 ± 0.25	0.12 ± 0.03	0.59 ± 0.11
Small Intestine	0.42 ± 0.07	0.53 ± 0.09	0.55 ± 0.05	1.57 ±0.28	0.26 ± 0.07	0.10 ± 0.03	0.30 ± 0.03
Large Intestine	-	0.25 ± 0.01	0.23 ± 0.05	0.82 ± 0.22	0.18 ± 0.09	0.31 ± 0.10	0.13 ± 0.02
Spleen	23.4 ± 6.40	3.14 ± 1.43†	0.45 ± 0.10†	20.6 ± 7.77	0.23 ± 0.02	0.07 ± 0.01	0.13 ± 0.03
Liver	0.45 ± 0.07	0.55 ± 0.10	0.62 ± 0.06	2.19 ± 0.34	0.23 ± 0.09	0.14 ± 0.03	0.24 ± 0.04
Pancreas	1.29 ± 0.94	0.48 ± 0.13	0.31 ± 0.02	2.20 ± 0.28	0.13 ± 0.07	0.04 ± 0.01	0.11 ± 0.03
Stomach	0.13 ± 0.01	0.25 ± 0.10	0.20 ± 0.03	0.55 ± 0.16	0.22 ± 0.07	0.16 ± 0.03	0.25 ± 0.02
Kidneys	45.3 ± 20.5	91.8 ± 29.1†	4.75 ± 0.43†	65.9 ± 5.10	15.0 ± 14.7†	1.95 ± 1.41	1.17 ± 0.16†
Lungs	3.64 ± 1.10	1.85 ± 0.23	1.19 ± 0.12	4.42 ± 0.47	0.42 ± 0.18	0.11 ± 0.03	0.38 ± 0.08
Heart	0.64 ± 0.10	0.56 ± 0.11	0.56 ± 0.08	2.65 ± 0.42	0.13 ± 0.05	0.04 ± 0.01	0.17 ± 0.02
LNCaP Tumor	10.3 ± 2.76	18.8 ± 6.71†	2.11 ± 0.16†	5.36 ± 1.18	9.48 ± 3.42†	7.58 ± 2.48	0.45 ± 0.09†
Muscle	0.45 ± 0.13	0.28 ± 0.07	0.31 ± 0.12	0.98 ± 0.16	0.08 ± 0.05	0.03 ± 0.02	0.10 ± 0.03
Bone	0.47 ± 0.13	0.53 ± 0.08	0.39 ± 0.14	0.79 ± 0.30	0.13 ± 0.07	0.05 ± 0.02	0.14 ± 0.03
Brain	0.03 ± 0.01	0.05 ± 0.01	0.04 ± 0.00	0.04 ± 0.01	0.02 ± 0.01	0.01 ± 0.00	0.02 ± 0.00
Salivary Glands	7.77 ± 3.01	2.35 ± 0.15†	0.71 ± 0.34†	19.1 ± 4.05	0.25 ± 0.19	0.06 ± 0.01	0.17 ± 0.13
Tumor/Bone	22.3 ± 6.16	35.8 ± 12.4	5.96 ± 2.34	7.43 ± 2.48	80.7 ± 42.7	164 ± 48.3	3.29 ± 0.73
Tumor/Muscle	21.8 ± 0.87	71.1 ± 28.9	7.32 ± 2.07	5.70 ± 2.05	97.0 ± 42.9	286 ± 103	4.82 ± 1.52
Tumor/Blood	15.4 ± 2.13	14.5 ± 5.55	1.08 ± 0.21	6.88 ± 2.16	18.5 ± 3.54	61.2 ± 15.0	0.75 ± 0.04
Tumor/Kidney	0.33 ± 0.14	0.21 ± 0.07	0.45 ± 0.02	0.08 ± 0.02	0.87 ± 0.39	4.56 ± 1.45	0.39 ± 0.03

†$p < 0.05$ between blocking and unblocked studies of candidates

2.4. In vivo stability

In vivo stability studies were conducted for all of the investigated tracers, and mouse plasma and urine samples (n = 3) were collected at 15 min post-injection for radio-HPLC analysis to check their intact fractions (Figures S1-S4). The intact fractions in urine and plasma samples were comparable for both [^{99m}Tc]Tc-EDDA-HTK03180 (84.2 ± 5.9% vs 82.2 ± 0.5%, Figure S2) and [^{99m}Tc]Tc-EDDA-KL01099 (67.3 ± 26.7% vs 72.9 ± 5.6%, Figure S3). However, a higher intact fraction in urine samples than in plasma samples was observed for both [^{99m}Tc]Tc-EDDA/HYNIC-iPSMA (87.2 ± 3.1% vs 14.9 ± 3.8%, Figure S1) and [^{99m}Tc]Tc-EDDA-KL01127 (84.7 ± 8.5% vs 32.1 ± 6.6%, Figure S4).

3. Discussion

High uptake of Lys-urea-Glu-derived PSMA-targeted radioligands in normal organs/tissues (such as kidneys, salivary glands, liver and spleen) hinders the detection of PCa lesions [17], and could potentially cause toxicity when radiotherapeutic agents are used [18]. Accumulated evidence has suggested that the high uptake of Lys-urea-Glu-derived PSMA-targeted radioligands in kidneys and salivary glands might be due to binding to off targets [19–21]. However, the identity of off-targets in kidneys and salivary glands remains controversial [22,23]. Recently we discovered that replacing Glu in the Lys-urea-Glu pharmacophore of [^{68}Ga]Ga-PSMA-617 with a close analog Aad led to [^{68}Ga]Ga-HTK03149 (Figure 1) with minimal uptake in kidneys and salivary glands [11]. Therefore, in this report, we investigated if the same phenomenon could be observed for the design of ^{99m}Tc-labeled HYNIC-conjugated PSMA-targeted tracers.

In vitro competition binding assays showed that reduced average K_i(PSMA) values were observed when replacing the Glu in the Lys-urea-Glu pharmacophore with Aad (3.11 nM for HYNIC-iPSMA vs 8.96 nM for KL01027; 10.7 nM for KL01099 vs 11.6 for HTK03180). This is consistent with our previous observation when comparing the Glu-containing Ga-HTK03041 (Figure 1, K_i(PSMA)= 0.63 nM) with the Aad-containing HTK03149 (Figure 1, K_i(PSMA)= 6.99 nM, Figure 1) [11,16]. These

Preprints (www.preprints.org) | NOT PEER-REVIEWED | Posted: 8 June 2023 doi:10.20944/preprints202306.0605.v1

data supports that compared with Aad, the Glu in the Lys-urea-Glu pharmacophore fits better into the glutamate pocket of the PSMA binding site. Previously we noticed that tranexamic acid in the lipophilic linker is important for maintaining high PSMA binding affinity [15], and replacing the 2-naphthyalanine in Ga-PSMA-617 with 9-anthrylalanine also improved PSMA binding affinity [16]. However, replacing the 2-naphthyalanine in HYNIC-iPSMA with 9-anthrylalanine and the addition of a tranexamic acid between HYNIC and 9-anthrylalanine did not lead to better PSMA binding affinity (K_i = 3.11 nM for HYNIC-iPSMA and 10.7 nM for KL01099). Similarly, the same phenomenon was observed when comparing the K_i values of KL01127 and HTK03180 (8.96 vs 11.6 nM). These data suggest that compared with HYNIC-tranexamic acid-9-anthrylalanine, HYNIC-2-naphthyalanine fits better into the S1 lipophilic accessory site of PSMA. In addition, the effect of modifying the lipophilic linker on PSMA binding affinity has to be considered based on the overall structure rather than the individual component of the lipophilic linker.

$LogD_{7.4}$ measurements revealed that replacing the bicyclic 2-naphthyalanine with a tricyclic 9-anthrylalanine and the addition of a tranexamic acid increased the overall lipophilicity of the radioligands ($LogD_{7.4}$ = -3.31 for [^{99m}Tc]Tc-EDDA/HYNIC-iPSMA and -2.13 for [^{99m}Tc]Tc-EDDA-KL01099; $LogD_{7.4}$ = -3.37 for [^{99m}Tc]Tc-EDDA-KL01127 and -2.56 for [^{99m}Tc]Tc-EDDA-HTK03180). Despite a higher lipophilicity, the $logD_{7.4}$ values of [^{99m}Tc]Tc-EDDA-KL01099 and [^{99m}Tc]Tc-EDDA-HTK03180 are < -2.0, and therefore, both tracers are still considered relatively hydrophilic and they are expected to be excreted mainly via the renal pathway.

The SPECT images and biodistribution data of all the investigated tracers confirm the prediction from their low $LogD_{7.4}$ values as all of them were excreted mainly via the renal pathway. With a relatively higher lipophilicity, [^{99m}Tc]Tc-EDDA-KL01099 ($LogD_{7.4}$ = -2.13) showed a relatively higher average uptake in liver (2.19 vs 0.23 - 0.55 %ID/g), small intestine (1.57 vs 0.26 – 0.53 %ID/g) and large intestine (0.82 vs 0.18 – 0.25 %ID/g) than the other tracers at 1 h post-injection. The much lower uptake of Lys-urea-Aad-derived tracers ([^{99m}Tc]Tc-EDDA-KL01127 and [^{99m}Tc]Tc-EDDA-HTK03180) in spleen and salivary glands when compared with their corresponding Lys-urea-Glu derivatives ([^{99m}Tc]Tc-EDDA-HYNIC/iPSMA and [^{99m}Tc]Tc-EDDA-KL01099) is consistent with our previous findings when comparing the biodistribution data of [^{68}Ga]Ga-HTK03041 [15] and [^{68}Ga]Ga-HTK03149 [11]. This suggests that replacing Glu in the Lys-urea-Glu pharmacophore of PSMA-targeted tracers with Aad reduces their binding to the off-targets expressed in spleen and salivary glands. However, the higher kidney uptake of the Lys-urea-Aad-derived [^{99m}Tc]Tc-EDDA-HTK03180 (91.8 %ID/g at 1 h post-injection) than the Lys-urea-Glu-derived [^{99m}Tc]Tc-EDDA-KL01099 (65.9 %ID/g at 1 h post-injection) was unexpected. Assuming the binding affinity to off-targets expressed in kidneys has been reduced with the replacement of Glu with Aad, the higher kidney uptake of [^{99m}Tc]Tc-EDDA-HTK03180 than [^{99m}Tc]Tc-EDDA-KL01099 could be due to factors other than off-target binding, which remain to be further investigated.

Despite comparable PSMA binding affinity (8.96 – 11.6 nM), the tumor uptake values of the reported 3 new tracers at 1 h post-injection varies from 5.36 ± 1.18 %ID/g for [^{99m}Tc]Tc-EDDA-KL01099, 9.48 ± 3.42 %ID/g for [^{99m}Tc]Tc-EDDA-KL01127 to 18.8 ± 6.71 %ID/g for [^{99m}Tc]Tc-EDDA-HTK03180. This indicates besides PSMA binding affinity, other factors such as binding to off-targets and pharmacokinetics also contribute significantly to the overall tumor uptake of these tracers. Among these tracers, [^{99m}Tc]Tc-EDDA-KL01127 had only moderate uptake in LNCaP tumor xenografts. However, [^{99m}Tc]Tc-EDDA-KL01127 also had the lowest background uptake, leading to higher tumor-to-background (bone, muscle, blood and kidney) uptake ratios than those of other tracers including the clinically validated [^{99m}Tc]Tc-EDDA/HYNIC-iPSMA (Table 1) [9,24]. Therefore, [^{99m}Tc]Tc-EDDA-KL01127 is promising for clinical translation for use to detect PCa with SPECT. The tumor-to-background uptake ratios of [^{99m}Tc]Tc-EDDA-KL01127 further improved over time and the tumor-to-kidney ratio reached 4.55 ± 1.45 at 3 h post-injection. Due to the 6 h half-life of ^{99m}Tc, the patients injected with [^{99m}Tc]Tc-EDDA-KL01127 could potentially be imaged at a later time point to further enable the detection of PCa lesions adjacent or in kidneys.

Preprints (www.preprints.org) | NOT PEER-REVIEWED | Posted: 8 June 2023 doi:10.20944/preprints202306.0605.v1

4. Materials and Methods

4.1. Synthesis of HYNIC-conjugated PSMA-targeted ligands

HYNIC-conjugated PSMA-targeted ligands were constructed on Wang resin using solid-phase peptide synthesis approach on the AAPPTec (Louisville, KY, USA) Endeavor 90 peptide synthesizer or CEM Corporation (Matthews, NC, USA) Liberty Blue automated microwave peptide synthesizer. *t*-Butyl protected Lys(ivDde)-urea-Glu and *t*-Butyl protected Lys(ivDde)-urea-Aad pharmacophores were first constructed on Wang resin following previously reported procedures [11,16,25]. The ivDde protecting group was removed with 5% hydrazine in DMF. Subsequent addition of Fmoc-protected linker and Boc-protected HYNIC chelator utilized 5 equivalents of amino acid derivative, 5 equivalents of HATU and 10 equivalents of DIPEA. Fmoc deprotection was conducted in between couplings with 20% piperidine in DMF. Ninhydrin tests were conducted to verify each coupling and deprotection steps. Final resin cleavage and deprotection was conducted using 95% trifluoroacetic acid and 5% triisopropylsilane for 4 h. After filtration, the crude peptides were precipitated by the addition of diethyl ether, centrifuged and purified by HPLC. The Agilent (Santa Clara, CA, USA) HPLC system consisted of a model 1200 quaternary pump and a model 1200 UV absorbance detector (set at 220 nm). The operation of the HPLC system was controlled by Agilent ChemStation software, and the HPLC column used was a semi-preparative column (Luna C18, 5 µm particle size, 100 Å pore size, 250 x 10 mm) purchased from Phenomenex (Torrance, CA, USA). The eluate fractions containing the desired product were collected, pooled, and lyophilized using a Labconco (Kansas City, MO, USA) FreeZone 4.5 Plus freeze drier. The identities of the PSMA-targeted ligands were verified by MS analysis using a Waters (Milford, MA, USA) Acquity QDa mass spectrometer with the equipped 2489 UV/Vis detector and e2695 Separations module. For HYNIC-iPSMA, the HPLC conditions were 20% acetonitrile and 0.1% formic acid in water and the flow rate was 4.5 mL/min. Its retention time was 9.7 min, and the yield was 34%. ESI-MS: calculated $[M+H]^+$ for $C_{31}H_{37}N_7O_9$ 652.3; found 652.3 (Figure S5). For HTK03180, the HPLC conditions were 27% acetonitrile and 0.1% formic acid in water and the flow rate was 4.5 mL/min. Its retention time was 9.3 min, and the yield was 32%. ESI-MS: calculated $[M+H]^+$ for $C_{44}H_{54}N_8O_{10}$ 855.4; found 855.6 (Figure S6). For KL01099, the HPLC conditions were 28% acetonitrile and 0.1% formic acid in water and the flow rate was 4.5 mL/min. Its retention time was 6.7 min, and the yield was 18%. ESI-MS: calculated $[M+H]^+$ for $C_{43}H_{52}N_8O_{10}$ 841.4; found 841.3 (Figure S7). For KL01127, the HPLC conditions were 20% acetonitrile and 0.1% formic acid in water and the flow rate was 4.5 mL/min. Its retention time was 9.8 min, and the yield was 36%. ESI-MS: calculated $[M+H]^+$ for $C_{40}H_{52}N_8O_{10}$ 666.3; found 666.2 (Figure S8).

4.2. Cell culture

The LNCaP cells obtained from ATCC (via Cedarlane, Burlington, Canada) were cultured in RPMI 1640 medium supplemented with 10% FBS, penicillin (100 U/mL) and streptomycin (100 µg/mL) at 37 °C in a Panasonic Healthcare (Tokyo, Japan) MCO-19AIC humidified incubator containing 5% CO_2. The cells were confirmed to be pathogen-free by the IMPACT Rodent Pathogen Test (IDEXX BioAnalytics, Columbia, MO, USA). Cells were grown until 80-90% confluence and washed with sterile phosphate-buffered saline (PBS, pH 7.4) and collected after 1 min trypsinization. The cell concentration was counted in triplicate using a hemocytometer and a manual laboratory counter.

4.3 In vitro competition binding assay

The *in vitro* competition binding assays were performed following our previously published procedures [15,26]. Briefly, LNCaP cells in RMPI medium with FBS, penicillin and streptomycin were plated onto 24-well poly-D-lysine coated plates at 200,000 cells/well 48 h prior to binding assay. Growth medium was removed and the cells were rinsed with HEPES buffered saline (50 mM HEPES, pH 7.5, 0.9% NaCl) two times before 400 µL of HEPES buffer was added to each well. Varying concentrations of PSMA-targeted ligands (50 µL) were added to each well in triplicates before adding 0.1 nmol/50 µL of [^{18}F]DCFPyL. After the additions, plates were incubated and swirled at 37 °C. After

Preprints (www.preprints.org) | NOT PEER-REVIEWED | Posted: 8 June 2023 doi:10.20944/preprints202306.0605.v1

1 h incubation, the solutions were removed and cells were washed with HEPES buffered saline twice. Finally, 400 µL of 0.25% trypsin solution was added to each well. After 10 min incubation, cells were collected for counting using a PerkinElmer (Waltham, MA, USA) Wizard2 2480 automatic gamma counter. The K_i values were analyzed with the GraphPad (San Diego, CA, USA) Prism 7 software using nonlinear regression fit.

4.4. Tc-99m labeling

HYNIC-conjugated ligand (5 nmol) in ACN/H_2O (according to previous HPLC purification conditions) was added to a mixture of EDDA (500 µg in 250 µL of 0.1 M NaOH), tricine (1 mg in 250 µL of 0.2 M PBS (pH = 6)) and $SnCl_2$ (400 µg in 20 µL of 0.1 M HCl), followed by the addition of around 740 MBq of [^{99m}Tc]$NaTcO_4$. The reaction mixture was incubated at 80 °C for 20 min, and then passed through a Waters (Milford, MA, USA) C18 Sep-Pak Plus Light cartridge (125 Å, 130 mg) which was pre-washed with ethanol (5 mL) and water (5 mL). The trapped Tc-99m labeled PSMA-targeted ligand was then eluted with ethanol (0.4 mL) and diluted with PBS to < 10% ethanol content for further studies. Quality control was performed on an Agilent HPLC system consisted of a model 1200 quaternary pump, a model 1200 UV absorbance detector (set at 220 nm), and a Bioscan (Washington DC, USA) NaI scintillation detector. The operation of the HPLC system was controlled by Agilent ChemStation software, and the HPLC column used was an analytical column (Luna C18, 5 µm particle size, 100 Å pore size, 250 x 4.6 mm) purchased from Phenomenex. The HPLC conditions were 0-80 % acetonitrile (over 20 min) and 0.1% formic acid in water and the flow rate was 2.0 mL/min. The retention times for Tc-99m labeled HYNIC-iPSMA, HTK03180, KL01099 and KL01127 were 11.1, 12.9, 12.9 and 11.1 min, respectively.

4.5. $LogD_{7.4}$ measurement

$LogD_{7.4}$ values were measured using the shake flask method as previously reported [15]. Briefly, an aliquot of Tc-99m labeled tracer (~1.85 MBq) was added to a vial containing 3 mL of *n*-octanol and 3 mL of phosphate buffer (0.1 M, pH 7.4). The mixture was vortexed for 2 min and then centrifuged at 3,000 rpm for 15 min. A sample (0.1 mL) of the n-octanol and buffer layers was counted using the Perkin Elmer Wizard2 2480 automatic gamma counter. Values of $LogD_{7.4}$ were calculated using the following equation: $LogD_{7.4} = \log_{10}$ [(counts in *n*-octanol phase)/(counts in buffer phase)].

4.6. Ex vivo biodistribution and SPECT/CT imaging studies

Ex vivo biodistribution and imaging studies were performed using male NOD-Rag1^{null}IL2rg^{null} (NRG) mice according to the guidelines established by the Canadian Council on Animal Care and approved by Animal Ethics Committee of the University of British Columbia. Mice were inoculated subcutaneously with 1.0×10^7 LNCaP cells in the left shoulder while under anesthesia (2% isoflurane in oxygen). The mice were then used for biodistribution and imaging studies around 5-6 weeks after inoculation.

SPECT/CT imaging experiments were conducted using the MILabs (Houten, The Netherlands) U-SPECT-II/CT scanner. Approximately 20 MBq of tracer was injected into LNCaP tumor-bearing mice via a lateral caudal tail vein and the mice were imaged at 1 h post-injection. For imaging, mice were sedated with 2% isoflurane in oxygen and positioned in the scanner on a heating pad with vitals monitored. For each image, a CT scan ran for 5 min to correct for localization and attenuation with voltage setting at 60 kV and current at 615 µA followed by a 60 min static emission scan acquired in list mode using an extra ultra high sensitivity multi-pinhole big mouse (2 mm pinhole size) collimator. Data was reconstructed using MILabs reconstruction software centered on the 140 keV photon peak. Reconstruction parameters used similarity regulated ordered subset expectation maximization (32 subsets, 10 iterations) and a post-processing filter (Gaussian blurring) of 0.6 mm. Scatter correction was performed using the automatic triple energy window setting and a calibration factor was applied generating images in MBq/mL. Images were decay corrected to injection time and divided by the injected activity in PMOD (PMOD Technologies, ZH) to obtain quantitative images expressed as the percentage of the injected dose per gram of tissue (%ID/g). Data

 doi:10.20944/preprints202306.0605.v1

was then converted to DICOM for visualization using Inveon Research Workplace (Siemens Healthineers, Erlangen, Germany).

For *ex vivo* biodistribution studies, mice were injected with ~2 MBq of tracer via tail vein. For blocking studies mice were co-injected with 0.5 mg of 2-PMPA. At the pre-determined time points, mice were euthanized by CO_2 asphyxiation. Blood and organs/tissues of interest were collected, weighted, and counted using the Perkin Elmer Wizard2 2480 automatic gamma counter.

4.7. in vivo stabilization

Male NRG mice (n = 3) were injected with ~10 MBq of Tc-99m labeled tracer and then euthanized at 15 min post-injection. Blood samples were collected via cardiac puncture and serum proteins were precipitated with the addition of equal volume of acetonitrile. The mixtures were centrifuged for 15 min to collect the clear plasma samples. Urine samples were also collected. Samples were filtered through a 0.45 micron filter, and analyzed by HPLC using the same conditions for the quality control of Tc-99m labeled tracers.

4.8. Statistical analysis

Statistical analyses were conducted using *t*-test or ANOVA using the Microsoft (Redmond, WA, USA) Excel software. A statistically significant difference was considered present when the adjusted P value was less than 0.05.

5. Conclusions

Replacing Glu in the Lys-urea-Glu pharmacophore of [^{99m}Tc]Tc-EDDA/HYNIC-iPSMA and [^{99m}Tc]Tc-EDDA-KL01099 generated [^{99m}Tc]Tc-EDDA-KL01127 and [^{99m}Tc]Tc-EDDA-KL03180, respectively, with greatly reduce off-target uptake in spleen and salivary glands. Compared with the clinically validated [^{99m}Tc]Tc-EDDA/HYNIC-iPSMA, its Lys-urea-Aad analog, [^{99m}Tc]Tc-EDDA-KL01127, showed comparable tumor uptake but greatly reduced off-target uptake in most of normal organs/tissues including spleen, kidneys and salivary glands, leading to superior tumor-to-background contrast ratios. [^{99m}Tc]Tc-EDDA-KL01127 is, therefore, promising for clinical translation for SPECT imaging to detect PCa lesions, and the Lys-urea-Aad pharmacophore is also promising for the design of PSMA-targeted ligands especially for radiotherapeutic application to minimize toxicity due to off-target uptake in normal organs/tissues.

6. Patents

Intellectual property rights related to compounds described in this manuscript have been licensed to Alpha-9 Theranostics, Inc.

Supplementary Materials: The following supporting information can be downloaded at the website of this paper posted on Preprints.org, Figure S1: Representative radio-HPLC chromatograms of plasma and urine samples collected at 15 min post-injection from mice injected with [^{99m}Tc]Tc-EDDA/HYNIC-iPSMA; Figure S2: Representative radio-HPLC chromatograms of plasma and urine samples collected at 15 min post-injection from mice injected with [^{99m}Tc]Tc-EDDA-HTK03180; Figure S3: Representative radio-HPLC chromatograms of plasma and urine samples collected at 15 min post-injection from mice injected with [^{99m}Tc]Tc-EDDA-KL01099; Figure S4: Representative radio-HPLC chromatograms of plasma and urine samples collected at 15 min post-injection from mice injected with [^{99m}Tc]Tc-EDDA-KL01127; Figure S5: A representative MS spectrum of HYNIC-iPSMA; Figure S6: A representative MS spectrum of HTK03180; Figure S7: A representative MS spectrum of KL01099; Figure S8: A representative MS spectrum of KL01127.

Author Contributions: Conceptualization, K.-S.L.; methodology, K.L., C.Z., Z.Z., H.-T.K., and N.C.; validation, K.L., C.Z. Z.Z., H.-T.K., N.C., and K.-S.L.; formal analysis, K.L. and Z.Z.; investigation, K.L., C.Z., N.C., H.-T.K., and Z.Z.; resources, F.B. and K.-S.L.; data curation, K.L., Z.Z., N.C., and K.-S.L.; writing—original draft preparation, K.L.; writing—review and editing, K.-S.L.; visualization, K.L.; supervision, K.-S.L. and F.B.; project administration, K.-S.L.; funding acquisition, K.-S.L. and F.B. All authors have read and agreed to the published version of the manuscript.

 doi:10.20944/preprints202306.0605.v1

Funding: This research was funded by Canadian Institute of Health Research (PJT-162243, PJT-180299 and PJT-180300).

Institutional Review Board Statement: The animal study protocol (A20-0113) was approved by the Animal Ethics Committee of the University of British Columbia on September 30, 2020.

Informed Consent Statement: Not applicable

Data Availability Statement: The data generated from this study are available in the text and in the Supplementary Materials.

Acknowledgments: We thank Helen Merkens for her help with animal acquisition and maintenance, and Ruiyan Tan and Ryan Wilson for their help with biodistribution studies.

Conflicts of Interest: F.B. and K.-S.L. are co-founders and consultants of Alpha-9 Theranostics Inc., and receive research funding from the company. H.-T.K. is a part-time employee of Alpha-9, and C.Z. and Z.Z. are also consultants for the company. F.B., K.-S.L., C.Z., H.-T.K. and Z.Z. hold shares and/or options in Alpha-9. The funders had no role in the design of the study; in the collection, analyses, or interpretation of data; in the writing of the manuscript; or in the decision to publish the results.

References

1. Wang, L.; Lu, B.; He, M.; Wang, Y.; Wang, Z.; Du, L. Prostate Cancer Incidence and Mortality: Global Status and Temporal Trends in 89 Countries From 2000 to 2019. *Front. Public Health* **2022**, *10*, 811044.
2. Bostwick, D.G.; Pacelli, A.; Blute, M.; Roche, P.; Murphy, G.P. Prostate Specific Membrane Antigen Expression in Prostatic Intraepithelial Neoplasia and Adenocarcinoma. *Cancer* **1998**, *82*, 2256–2261.
3. Hupe, M.C.; Philippi, C.; Roth, D.; Kümpers, C.; Ribbat-Idel, J.; Becker, F.; Joerg, V.; Duensing, S.; Lubczyk, V.H.; Kirfel, J.; et al. Expression of Prostate-Specific Membrane Antigen (PSMA) on Biopsies Is an Independent Risk Stratifier of Prostate Cancer Patients at Time of Initial Diagnosis. *Front. Oncol.* **2018**, *8*, 623.
4. Evans, M.J.; Smith-Jones, P.M.; Wongvipat, J.; Navarro, V.; Kim, S.; Bander, N.H.; Larson, S.M.; Sawyers, C.L. Noninvasive Measurement of Androgen Receptor Signaling with a Positron-Emitting Radiopharmaceutical That Targets Prostate-Specific Membrane Antigen. *Proc. Natl. Acad. Sci. U.S.A.* **2011**, *108*, 9578–9582.
5. Heston, W.D. Characterization and Glutamyl Preferring Carboxypeptidase Function of Prostate Specific Membrane Antigen: A Novel Folate Hydrolase. *Urology* **1997**, *49*, 104–112.
6. Davis, M.I.; Bennett, M.J.; Thomas, L.M.; Bjorkman, P.J. Crystal Structure of Prostate-Specific Membrane Antigen, a Tumor Marker and Peptidase. *Proc. Natl. Acad. Sci. U.S.A.* **2005**, *102*, 5981–5986.
7. Tsukamoto, T.; Wozniak, K.M.; Slusher, B.S. Progress in the Discovery and Development of Glutamate Carboxypeptidase II Inhibitors. *Drug Discovery Today* **2007**, *12*, 767–776.
8. Kozikowski, A.P.; Zhang, J.; Nan, F.; Petukhov, P.A.; Grajkowska, E.; Wroblewski, J.T.; Yamamoto, T.; Bzdega, T.; Wroblewska, B.; Neale, J.H. Synthesis of Urea-Based Inhibitors as Active Site Probes of Glutamate Carboxypeptidase II: Efficacy as Analgesic Agents. *J. Med. Chem.* **2004**, *47*, 1729–1738.
9. Ferro-Flores, G.; Luna-Gutiérrez, M.; Ocampo-García, B.; Santos-Cuevas, C.; Azorín-Vega, E.; Jiménez-Mancilla, N.; Orocio-Rodríguez, E.; Davanzo, J.; García-Pérez, F.O. Clinical Translation of a PSMA Inhibitor for ^{99m}Tc-Based SPECT. *Nucl. Med. Biol.* **2017**, *48*, 36–44.
10. Santos-Cuevas, C.; Davanzo, J.; Ferro-Flores, G.; García-Pérez, F.O.; Ocampo-García, B.; Ignacio-Alvarez, E.; Gómez-Argumosa, E.; Pedraza-López, M. ^{99m}Tc-Labeled PSMA Inhibitor: Biokinetics and Radiation Dosimetry in Healthy Subjects and Imaging of Prostate Cancer Tumors in Patients. *Nucl. Med. Biol.* **2017**, *52*, 1–6.

11. Kuo, H.-T.; Lin, K.-S.; Zhang, Z.; Zhang, C.; Merkens, H.; Tan, R.; Roxin, A.; Uribe, C.F.; Bénard, F. What a Difference a Methylene Makes: Replacing Glu with Asp or Aad in the Lys-Urea-Glu Pharmacophore of PSMA-Targeting Radioligands to Reduce Kidney and Salivary Gland Uptake. *Theranostics* **2022**, *12*, 6179–6188.
12. Decristoforo, C.; Mather, S.J. 99m-Technetium-Labelled Peptide-HYNIC Conjugates: Effects of Lipophilicity and Stability on Biodistribution. *Nucl. Med. Biol.* **1999**, *26*, 389–396.
13. King, R.C.; Surfraz, M.B.-U.; Biagini, S.C.G.; Blower, P.J.; Mather, S.J. How Do HYNIC-Conjugated Peptides Bind Technetium? Insights from LC-MS and Stability Studies. *Dalton Trans.* **2007**, *43*, 4998–5007.
14. Guggenberg, E.V.; Mikolajczak, R.; Janota, B.; Riccabona, G.; Decristoforo, C. Radiopharmaceutical Development of a Freeze-Dried Kit Formulation for the Preparation of [^{99m}Tc-EDDA-HYNIC-D-Phe^{1},Tyr^{3}]-Octreotide, a Somatostatin Analog for Tumor Diagnosis. *J. Pharm. Sci.* **2004**, *93*, 2497–2506.
15. Kuo, H.-T.; Lepage, M.L.; Lin, K.-S.; Pan, J.; Zhang, Z.; Liu, Z.; Pryyma, A.; Zhang, C.; Merkens, H.; Roxin, A.; et al. One-Step 18F-Labeling and Preclinical Evaluation of Prostate-Specific Membrane Antigen Trifluoroborate Probes for Cancer Imaging. *J. Nucl. Med.* **2019**, *60*, 1160–1166.
16. Kuo, H.-T.; Lin, K.-S.; Zhang, Z.; Uribe, C.F.; Merkens, H.; Zhang, C.; Bénard, F. ^{177}Lu-Labeled Albumin-Binder–Conjugated PSMA-Targeting Agents with Extremely High Tumor Uptake and Enhanced Tumor-to-Kidney Absorbed Dose Ratio. *J. Nucl. Med.* **2021**, *62*, 521–527.
17. Dietlein, F.; Kobe, C.; Neubauer, S.; Schmidt, M.; Stockter, S.; Fischer, T.; Schomäcker, K.; Heidenreich, A.; Zlatopolskiy, B.D.; Neumaier, B.; et al. PSA-Stratified Performance of ^{18}F- and ^{68}Ga-PSMA PET in Patients with Biochemical Recurrence of Prostate Cancer. *J. Nucl. Med.* **2017**, *58*, 947–952.
18. Kratochwil, C.; Bruchertseifer, F.; Giesel, F.L.; Weis, M.; Verburg, F.A.; Mottaghy, F.; Kopka, K.; Apostolidis, C.; Haberkorn, U.; Morgenstern, A. ^{225}Ac-PSMA-617 for PSMA-Targeted α-Radiation Therapy of Metastatic Castration-Resistant Prostate Cancer. *J. Nucl. Med.* **2016**, *57*, 1941–1944.
19. Rousseau, E.; Lau, J.; Kuo, H.-T.; Zhang, Z.; Merkens, H.; Hundal-Jabal, N.; Colpo, N.; Lin, K.-S.; Bénard, F. Monosodium Glutamate Reduces ^{68}Ga-PSMA-11 Uptake in Salivary Glands and Kidneys in a Preclinical Prostate Cancer Model. *J. Nucl. Med.* **2018**, *59*, 1865–1868.
20. Mhawech-Fauceglia, P.; Zhang, S.; Terracciano, L.; Sauter, G.; Chadhuri, A.; Herrmann, F.R.; Penetrante, R. Prostate-Specific Membrane Antigen (PSMA) Protein Expression in Normal and Neoplastic Tissues and Its Sensitivity and Specificity in Prostate Adenocarcinoma: An Immunohistochemical Study Using Mutiple Tumour Tissue Microarray Technique. *Histopathology* **2007**, *50*, 472–483.
21. Rupp, N.J.; Umbricht, C.A.; Pizzuto, D.A.; Lenggenhager, D.; Töpfer, A.; Müller, J.; Muehlematter, U.J.; Ferraro, D.A.; Messerli, M.; Morand, G.B.; et al. First Clinicopathologic Evidence of a Non–PSMA-Related Uptake Mechanism for ^{68}Ga-PSMA-11 in Salivary Glands. *J. Nucl. Med.* **2019**, *60*, 1270–1276.
22. Lee, Z.; Heston, W.D.; Wang, X.; Basilion, J.P. GCP III Is Not the "off-Target" for Urea-Based PSMA Ligands. *Eur. J. Nucl. Med. Mol. Imaging* **2023**, doi:10.1007/s00259-023-06265-6.
23. Lucaroni, L.; Georgiev, T.; Prodi, E.; Puglioli, S.; Pellegrino, C.; Favalli, N.; Prati, L.; Manz, M.G.; Cazzamalli, S.; Neri, D.; et al. Cross-Reactivity to Glutamate Carboxypeptidase III Causes Undesired Salivary Gland and Kidney Uptake of PSMA-Targeted Small-Molecule Radionuclide Therapeutics. *Eur. J. Nucl. Med. Mol. Imaging* **2023**, *50*, 957–961.
24. García-Pérez, F.O.; Davanzo, J.; López-Buenrostro, S.; Santos-Cuevas, C.; Ferro-Flores, G.; Jímenez-Ríos, M.A.; Scavuzzo, A.; Santana-Ríos, Z.; Medina-Ornelas, S. Head to Head Comparison Performance of ^{99m}Tc-EDDA/HYNIC-iPSMA SPECT/CT and ^{68}Ga-PSMA-11 PET/CT a Prospective Study in Biochemical Recurrence Prostate Cancer Patients. *Am. J. Nucl. Med. Mol. Imaging* **2018**, *8*, 332–340.

 doi:10.20944/preprints202306.0605.v1

25. Kuo, H.-T.; Pan, J.; Zhang, Z.; Lau, J.; Merkens, H.; Zhang, C.; Colpo, N.; Lin, K.-S.; Bénard, F. Effects of Linker Modification on Tumor-to-Kidney Contrast of ^{68}Ga-Labeled PSMA-Targeted Imaging Probes. *Mol. Pharmaceutics* **2018**, *15*, 3502–3511.
26. Kuo, H.-T.; Merkens, H.; Zhang, Z.; Uribe, C.F.; Lau, J.; Zhang, C.; Colpo, N.; Lin, K.-S.; Bénard, F. Enhancing Treatment Efficacy of ^{177}Lu-PSMA-617 with the Conjugation of an Albumin-Binding Motif: Preclinical Dosimetry and Endoradiotherapy Studies. *Mol. Pharmaceutics* **2018**, *15*, 5183–5191.